



# COMPUTATIONAL STUDIES ON AERO-THERMODYNAMIC DESIGN AND PERFORMANCE OF CENTRIFUGAL TURBO-MACHINERY

**Dr. CH V K N S N Moorthy, K Bharadwajan**

Department of Mechanical Engineering,  
Institute of Aeronautical Engineering (Autonomous), Hyderabad, Telangana, India

**Dr. V Srinivas**

Department of Mechanical Engineering, GITAM University,  
Vishakhapatnam, Andhra Pradesh, India

## ABSTRACT

*Compressor design of a gas driven turbo-machinery component, involves extensive iterative process with enormous complex three-dimensional flow phenomena embedded within a dynamic state-of-the-art multi flow physics posing many challenges to its aero-thermodynamic design and performance. The present work attempts to address above cited technical issues connecting both design and performance of a centrifugal compressor with backward swept blade profile producing total pressure ratio of 5.4 with an ingested mass flow rate of 5.73 kg/s. A Mean-line design methodology was implemented to configure sizing of the compressor. An optimum grid size was well validated by carrying out computational analysis with three different mesh sizes within the same framework. Finally, a detailed three dimensional numerical simulation was performed to validate polytropic efficiency, total-to-total efficiency, stagnation pressure ratio at a fixed rotational speed and the overall design aero-thermodynamic performance.*

**Key words:** Turbo-machinery, Centrifugal compressor, Aero-thermodynamics, Propulsion and Diffuser

**Cite this Article:** Dr. CH V K N S N Moorthy, K Bharadwajan and Dr. V Srinivas, Computational Studies on Aero-Thermodynamic Design and Performance of Centrifugal Turbo-Machinery. *International Journal of Mechanical Engineering and Technology*, 8(5), 2017, pp. 320–333.

<http://www.iaeme.com/IJMET/issues.asp?JType=IJMET&VType=8&IType=5>

## 1. INTRODUCTION

Centrifugal compressors find usage over wide range of propulsion applications and are regarded as one among the key air-breathing propulsive engine components. The cognitive research and development of compressors is directed towards achieving a higher pressure

ratio, higher efficiency and reduced structural weight of compressor and the engine as well. Various compressor stages achieve gradual increase in the stagnation-to-flow pressure contributed by flow diffusion. Energy is added in the rotor blade section, increasing the total pressure and absolute component of flow velocity. Stator blade row diffuses the flow, thus reducing absolute velocity component and elevating static pressure. Blade topology requires adaptation of a cautious design procedure to achieve the designated pressure rise while minimizing aero-thermodynamic losses in order to run and achieve design pressure ratios and design efficiencies.

## 2. CENTRIFUGAL COMPRESSOR SPECIFICATIONS

Main objective of the current work is to design a centrifugal compressor capable of delivering a pressure ratio of 5.4 and mass flow ingestion rate of 5.73 kg/sec. The compressor is targeted to achieve 82% total-total efficiency with design constraints of 280 mm for the impeller and 340 mm for diffuser in terms of diameter. Also, the compressor has to generate flow parameters relative to functional downstream components.

**Table 1** Geometrical and functional specifications of analyzed turbo-machinery

S. No	Name of the parameter	Value
1	Mass Flow Rate	5.73 kg/s
2	Pressure Ratio	5.4:1
3	Efficiency	82 %
4	Maximum Impeller Diameter	280mm
5	Maximum Diffuser Diameter	340mm
6	Rotational Speed	38000 rpm
7	Inlet Pressure	101325 Pa
8	Inlet Temperature	288.15 K

## 3. PRELIMINARY DESIGN

Algorithm for preliminary design procedure adapting a one dimensional model approach is represented in Figure 1.

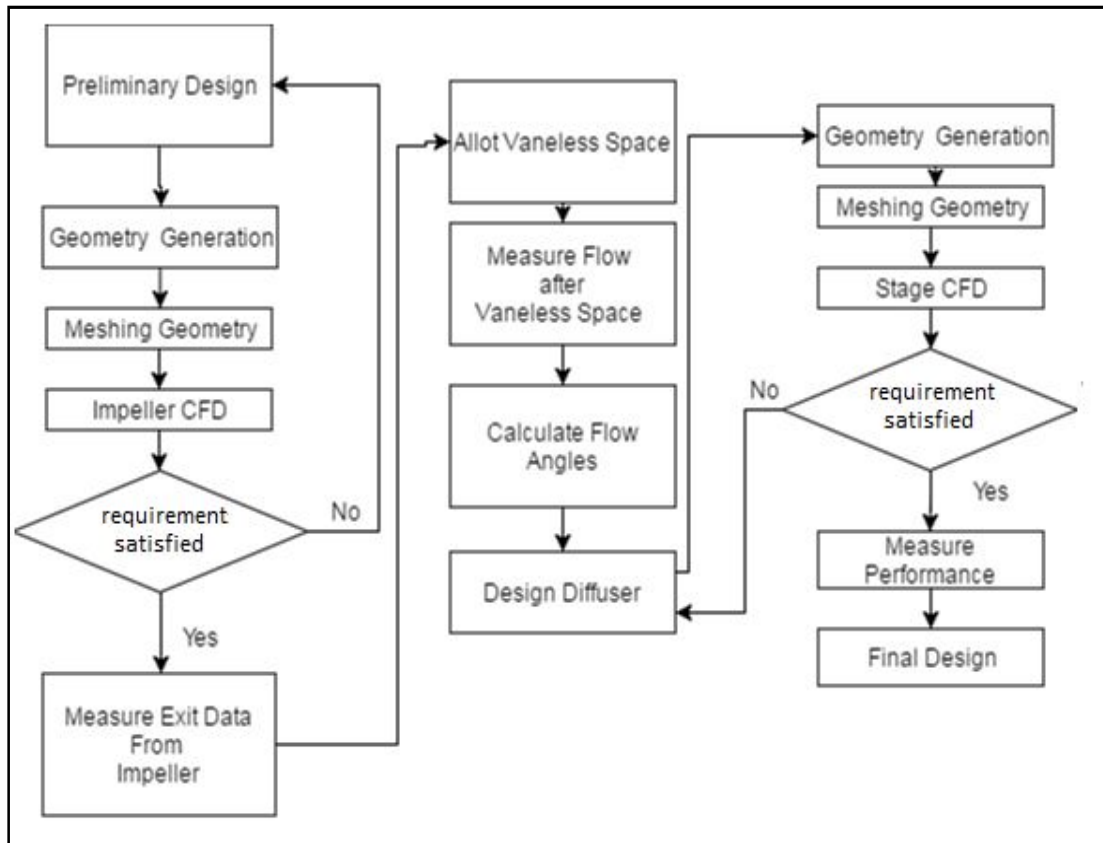


Figure 1 Algorithm for preliminary design

### 3.1. Impeller

There are various strategic geometric/design features to be identified and discussed with respect to impeller, its inlet and outlet design. In principal, aerodynamic losses occurring in majority of turbo-machines arise primarily due to the boundary layer growth, its separation on blade profile and passage surfaces termed as profile losses widely configured under primary losses.

Impeller was designed using guidelines from various sources and in specific from [1]. The number of impeller blade profiles was configured based upon a choice iterative method aiming for passage flow devoid of heavy separations and it was streamlined and set at 19 blade profiles. Figure 1 shows design procedure adapted for entire stage and a rotational speed of 38000 rpm was set for the impeller.

#### 3.1.1. Impeller Inlet

Hub-to-tip ratio is a key owing to the secondary losses, which occurs in the flow regions near the end walls. The presence of any undesirable circulatory or cross-flows develop on account of rapid and steep flow turning through the blade channel accounting for annulus wall boundary layers. Therefore, impeller hub-to-tip ratio was set at 0.35 within the range 0.3-0.6 prescribed in [1].

Mach number at impeller inlet was set at 0.65. Impeller inlet blade angles were setup by PCA Engineer's Vista CCD tool analytical calculations. The inducer leading edge angles are  $35^\circ$ ,  $56^\circ$  and  $63^\circ$  respectively with incidences of  $11.8^\circ$ ,  $3.7^\circ$ , and  $0.1^\circ$  at hub, mean, and shroud respectively. Leading edge of the impeller was defined by an elliptic ratio of 6.

### 3.1.2. Impeller Outlet

Impeller backswept angle was set at  $0^\circ$  to minimize impeller diameter and a lean angle of  $30^\circ$  was also incorporated into the design. Impeller exducer height at 13.7032 mm and impeller diameter of 257.954 mm was set by PCA Engineer's Vista CCD software impeller trailing edge was defined as a square cutoff.

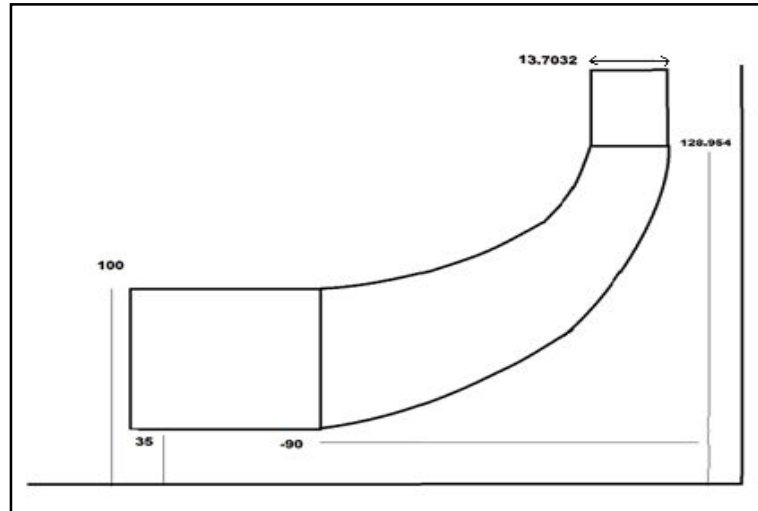


**Figure 2** Dimensions of the impeller

### 3.1.3. Vaned diffuser

In order to obtain higher pressure ratio in a radial diffuser, the diffusion process has to be achieved across a relatively shorter radial distance. This requires the application of vanes which provide greater guidance to flow inside diffusing passages. The vaned diffuser was designed by observing various flow parameters reflected at impeller exit after performing numerical simulations.

To circumvent flow separation, divergence of diffuser blade passages in vaned diffuser ring can be kept small incorporating large number of vanes. However, this can lead to higher friction losses. Thus an optimum number of diffuser vanes must be employed and flow passage divergence not to exceed  $12^\circ$ . Thus final diffuser design contains 30 blades. The diffuser vane leading edge was at a radius of 136 mm and the trailing edge of the diffuser vanes was set at radius of 166 mm. Blade inlets and outlet angle was set at  $64^\circ$ . The leading and trailing edge were defined by an elliptic ratio of 6 and radius of 0.25 mm.

Another method to prevent very steep velocity gradients at diffuser entry is by providing a small vane less space ( $0.05d_2-0.1d_2$ ) between impeller exit and diffuser entry. Therefore, a vane less space of 7.023 mm was allotted.

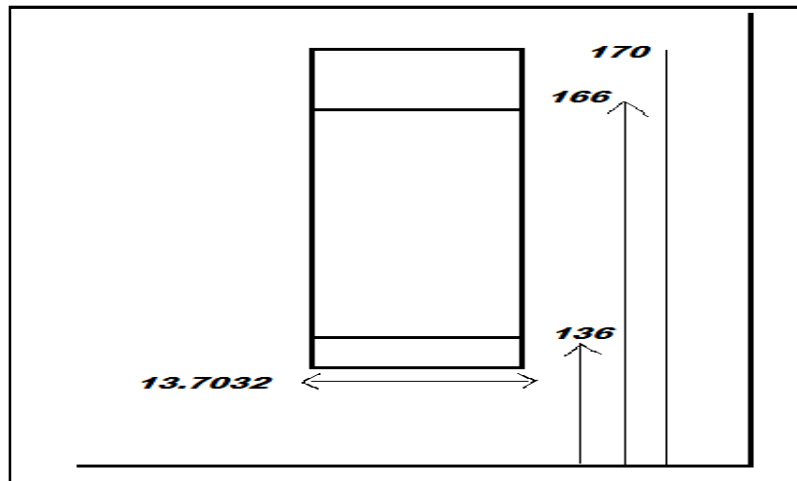


Figure 3 Drafted diffuser CAD Model

#### 4. DETAILED DESIGN

Comprehensive design of the centrifugal compressor stage was generated using Ansys-Bladegen module.

##### 4.1. Impeller

Data generated by Vista CCD tool was used to generate a 3D computer aided design model of impeller. Inlet portion of 50 mm and horizontal was designed satisfying diameter constraint of 280 mm.

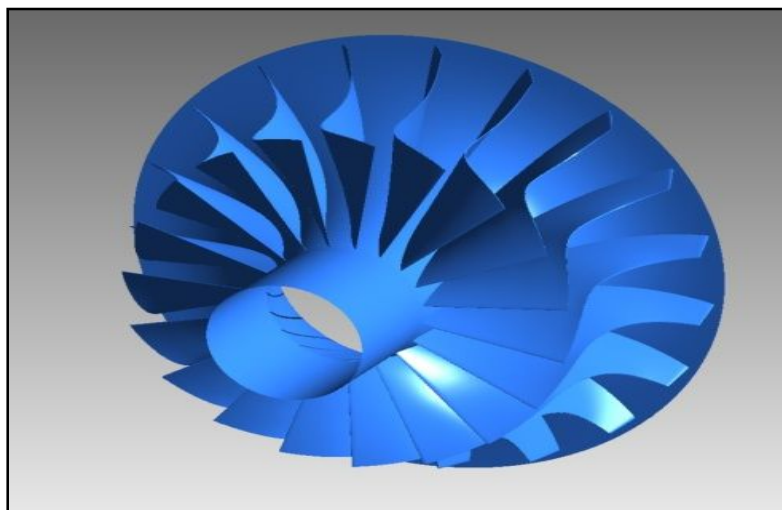
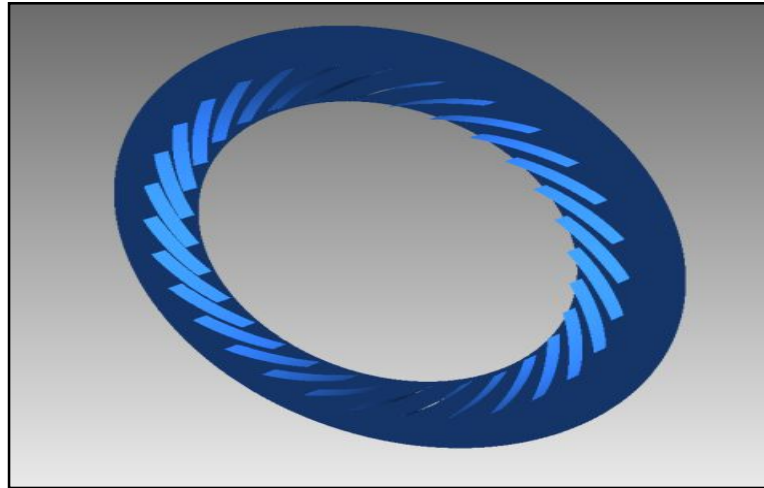


Figure 4 Three dimensional computer aided design of impeller model

##### 4.2. Vaned Diffuser

A discussion pertaining to importance of vaned diffuser in previous section, impeller leading-, and trailing-edges definitions were set accordingly and design of vaneless space was performed in Ansys-Bladegen. Diffuser vane profiles were designed and chosen using an iterative approach by performing diverse case study simulations with a choice of profiles.



**Figure 5** Three dimensional computer aided design of diffuser model

The design methodology adapted was mainly focused aiming at decrease of Mach number and flow angle at diffuser exit by satisfying diameter constraint of 340 mm.

## 5. MESHING

Adapted meshing strategy for both the impeller and diffuser fluid domains was achieved using Ansys-Turbogrid module. A total node count of 7e-01 million was setup for the CFD solver, as it allows generation of refined quality hexahedral meshes required for the blade passages in turbo-machinery.

## 6. NUMERICAL SETUP

In the present context, ANSYS CFX tool is setup with pressure based solver simulating a steady, three dimensional viscous flow fields using complete set of Navier-Stokes code solving for Reynolds-Averaged Navier-Stokes equations based on finite volume discretization method. A high resolution scheme is used to solve for continuity, momentum, energy and state equations implementing a standard k- $\epsilon$  turbulence model. Individual compressor stage characteristics were generated by performing simulations varying back pressures. Firstly, near choke condition flow points are run to reduced static back pressure values and later solutions are restarted with incrementally increasing the static back pressure to compute intermediate points on constant speed line running towards stall.

**Inlet Boundary Conditions:** At compressor inlet, a constant total pressure and total temperature conditions are imposed with a turbulence intensity of 1% and flow direction is marked normal to the inlet plane.

**Outlet Boundary Conditions:** At the outlet, an average static pressure boundary condition is implemented. Also, a circumferential symmetry condition is imposed on corresponding periodic surfaces with air fluid medium setup as an ideal gas. A counter-rotating wall boundary is given at the impeller shroud.

## 7. RESULTS AND DISCUSSIONS

### 7.1. Flow Analysis – Velocity Triangles

Entry and exit velocity triangles for impeller blades along the radial section with backward swept blades ( $\beta_2 = 0^\circ$ ) are plotted. Inlet Mach number is within the recommended range of 0.4 to 0.6.

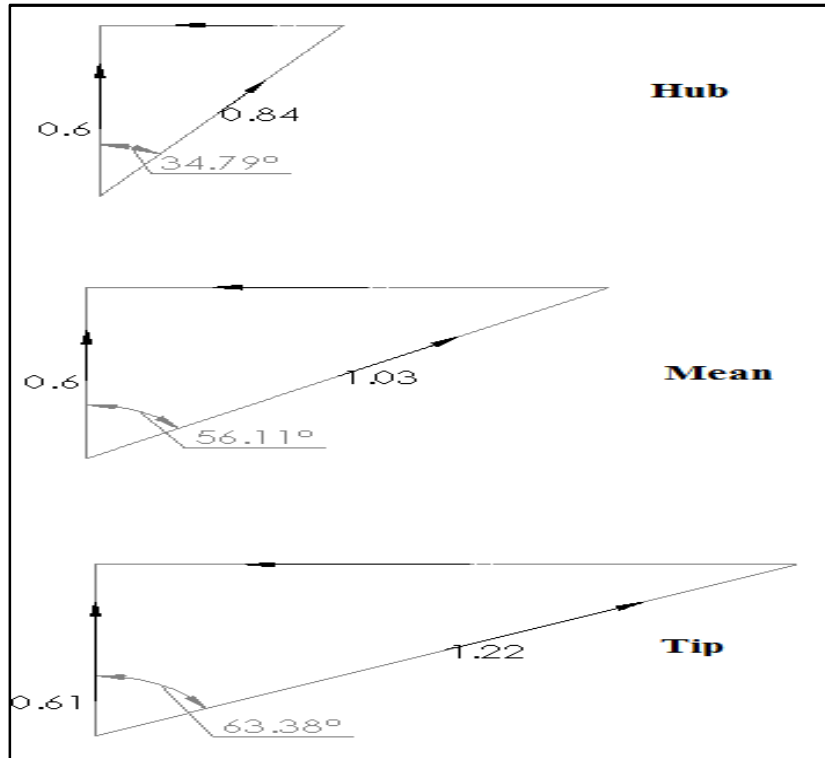


**Figure 6** Inlet Mach triangles for impeller blades only in radial section with backward swept blades,  $\beta_2 = 0^\circ$  with zero swirl at entry

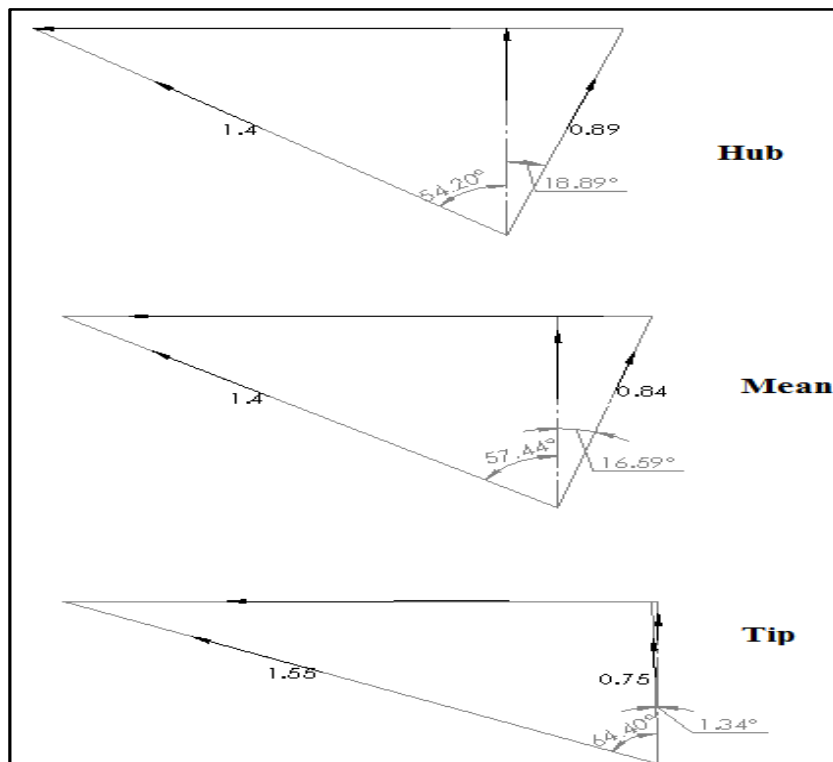


**Figure 7** Exit Mach triangles for impeller blades only in radial section with backward swept blades,  $\beta_2 = 0^\circ$  with zero swirl at entry

A maximum flow angle of  $64^\circ$  at the impeller exit and a mach number of 1.4 are observed.

## 7.2. Blade to Blade Contours

Blade to blade contours for absolute Mach number at hub, mean and tip sections are presented in below figures.

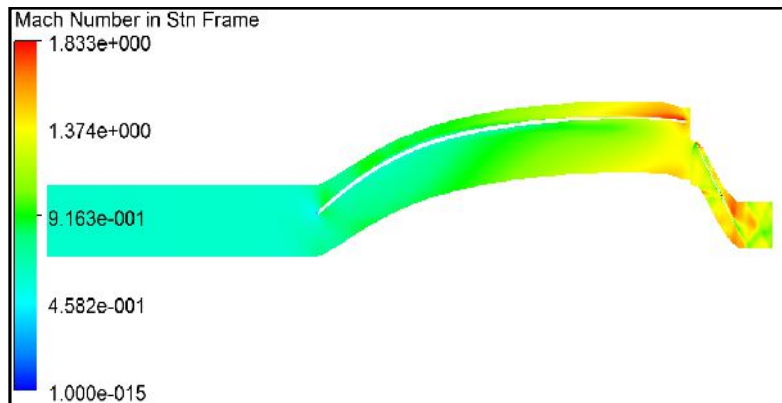


**Figure 8** Hub section absolute Mach number contour

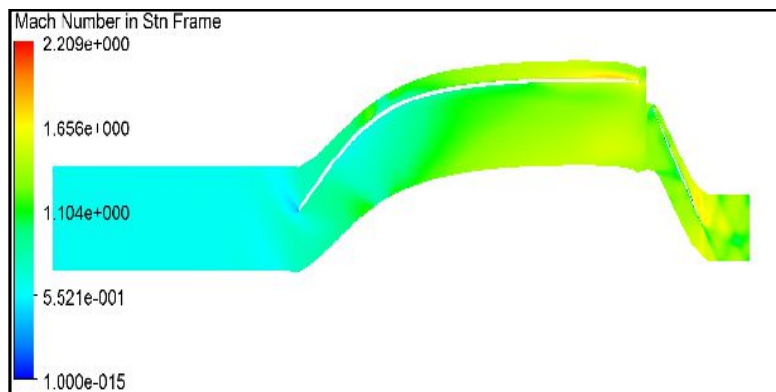


**Figure 9** Mean section absolute Mach number contour

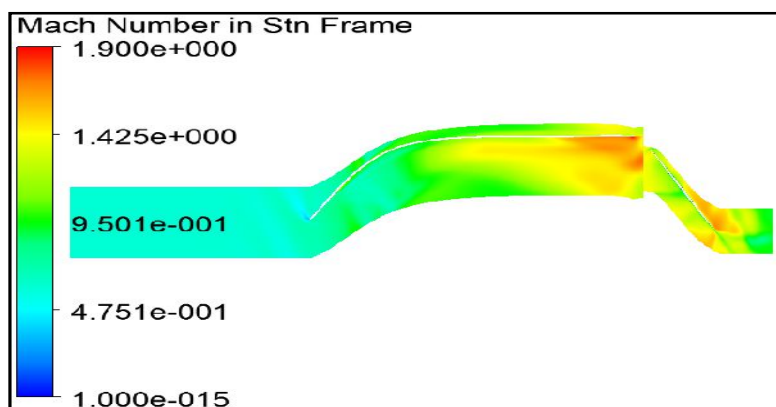


**Figure 10** Tip section absolute Mach number contour

The absolute Mach number plots show no supersonic regions of significant volume. The Hub section plot show supersonic flow near suction surface of the blade and the Tip Section span plots show a supersonic region on the pressure surface of the blade. The presence of a mild bow shock in front of the leading edge of the blade can also be observed. The Mach number is around 0.6 at the leading edge of the impeller. The following plot is the relative Mach number contour for the hub, mean and tip.

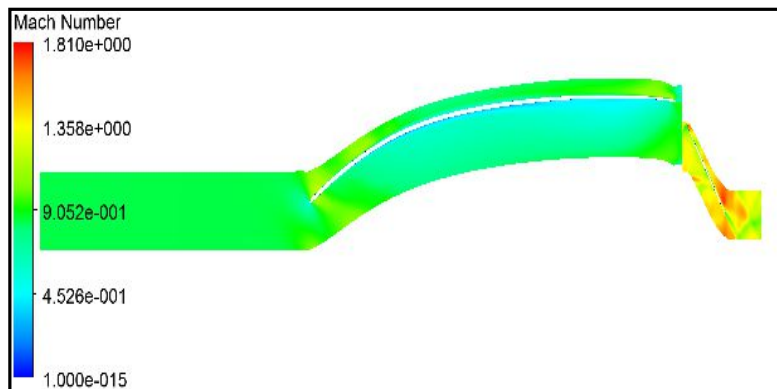


**Figure 11** Hub section relative Mach number contour

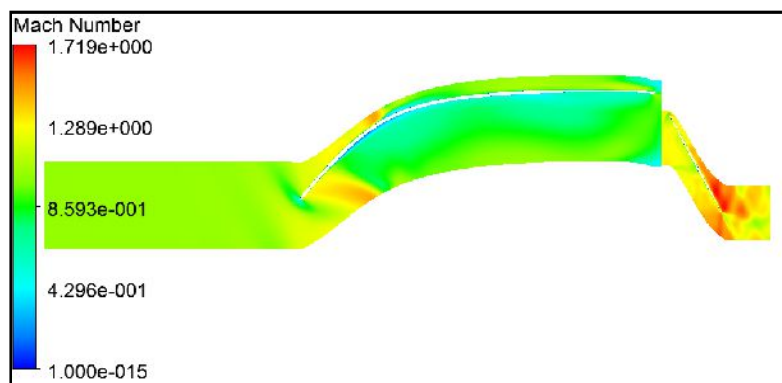


**Figure 12** Mean section relative Mach number contour

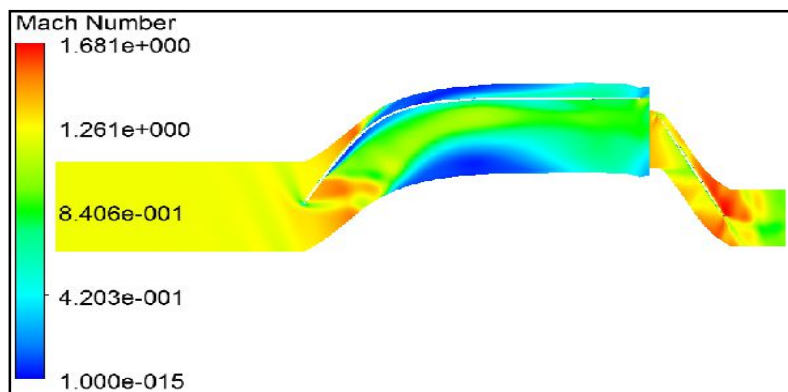


**Figure 13** Tip section relative Mach number contour

The Mach number at the leading edge in the relative frame is near 1.2 for the leading edge of the impeller blade. The regions of low Mach number can also be observed, although it is in the relative frame.

### 7.3. Circumferential Contour

Circumferential relative Mach number contours at the impeller inlet and outlet are presented below. The higher color temperature indicates higher values of Relative Mach number.

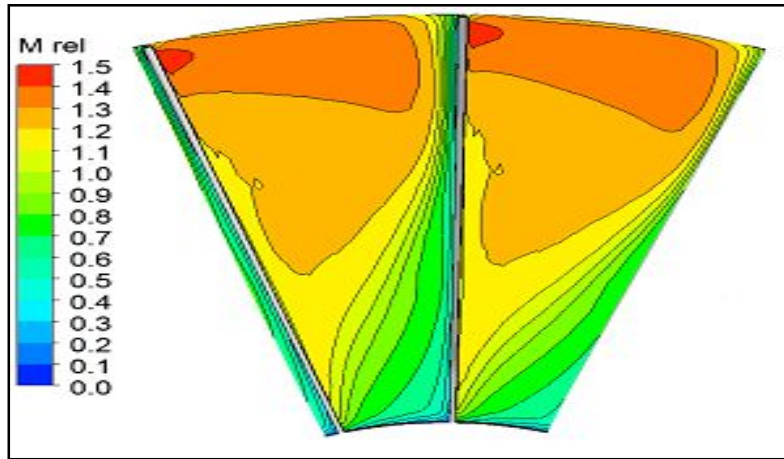


**Figure 14** Inlet Relative Mach Contour

From above figure 14, corresponding inlet relative Mach number contours shows that passage area is lying in the supersonic regime.

The figure 15 shows the contour map of the relative Mach number at the impeller outlet. The higher color temperature indicates higher values of Relative Mach number.

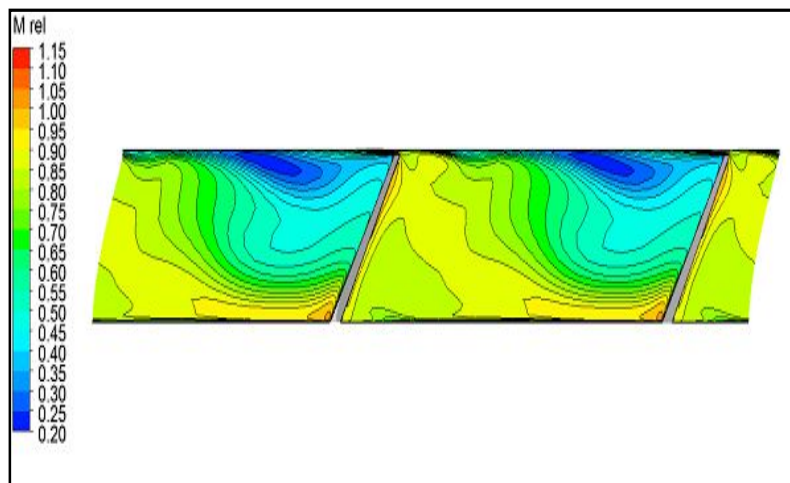


**Figure 15** Outlet Relative Mach Contour

From above relative mach contour, the effect of lean angle of impeller blades can be observed.

#### **7.4. Performance Characteristics**

Individual component as well as stage performance as a whole can be gauged by different methods.

##### **7.4.1. Impeller Performance Characteristics**

Impeller performance was evaluated by Vista-CCM and their corresponding plots are shown in below figures. Fig 18 represents the variation of pressure ratio with varying mass flow ingested through compressor.

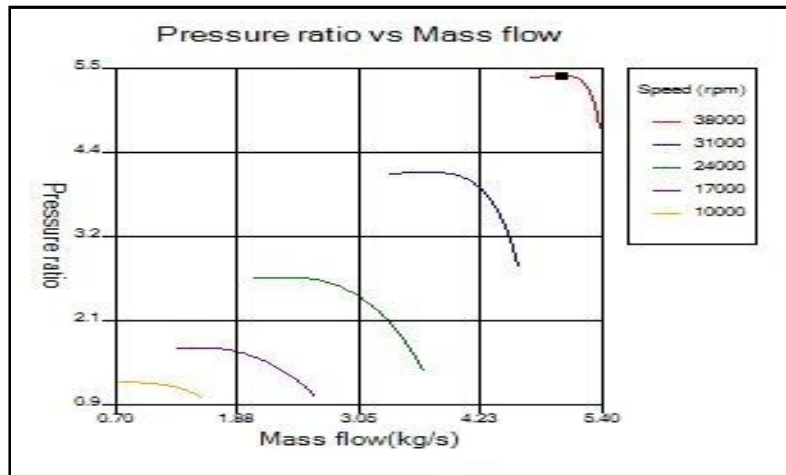


**Figure 16** Mass flow versus Pressure Ratio by Vista CCM

Figure 17 represents the variation of polytropic efficiency with varying mass flow ingested to quantify differential pressure changes occurring through compressor stage.

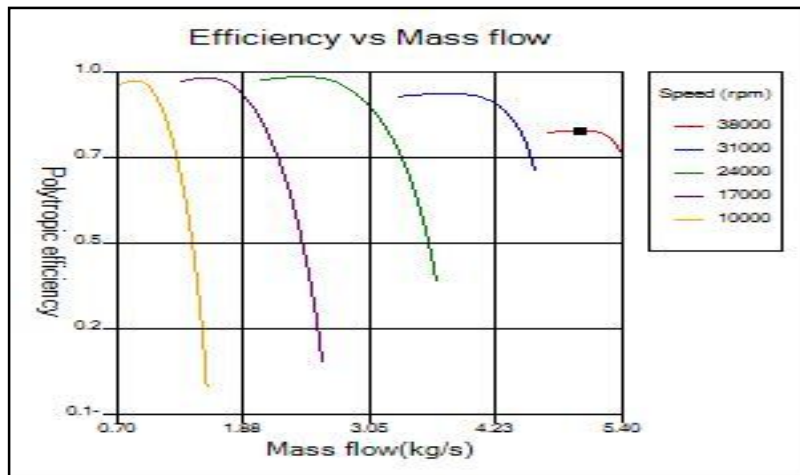


**Figure 17** Mass flow versus Polytropic Efficiency by Vista CCM

#### 7.4.2. Stage Performance Characteristics

Compressor stage performance can be evaluated by obtaining individual characteristic curves as plotted in Figures 18-20. The compressor performance is presented only for a functional design speed of 38000 rpm. Variables like total pressure ratio, adiabatic efficiency, and power requirement of compressor are plotted against varying mass flow rate. The maximum achieved pressure ratio is 5.4 while allowing a fixed mass flow rate of 5.73 kg/s.

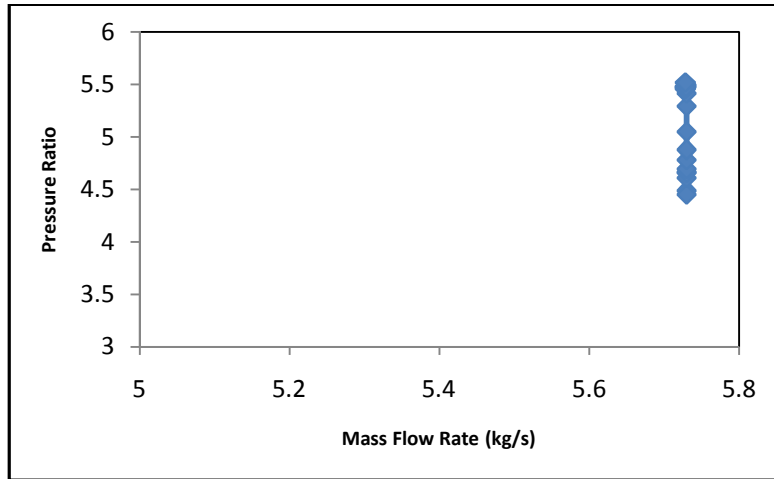


**Figure 18** Pressure Ratio versus Mass Flow

A peak efficiency of 75.8% is obtained at a pressure ratio of 5.73. The design point efficiency is predicted to be around 74.5%. Possible reasons for loss in efficiency may be owing to primary and secondary losses.

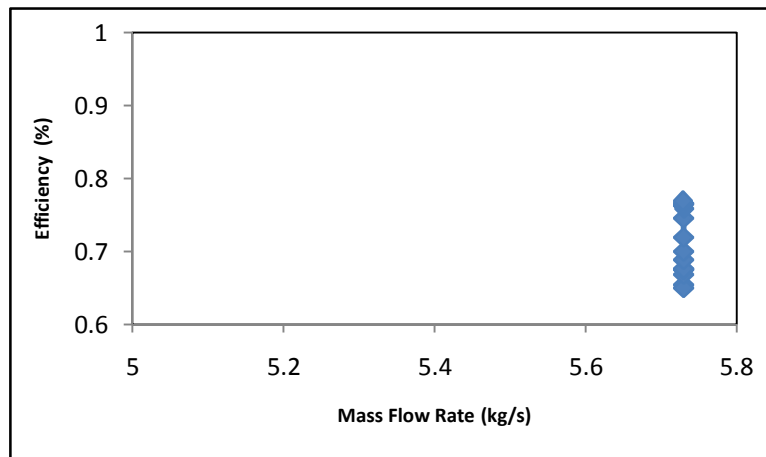


**Figure 19** Efficiency versus Mass Flow

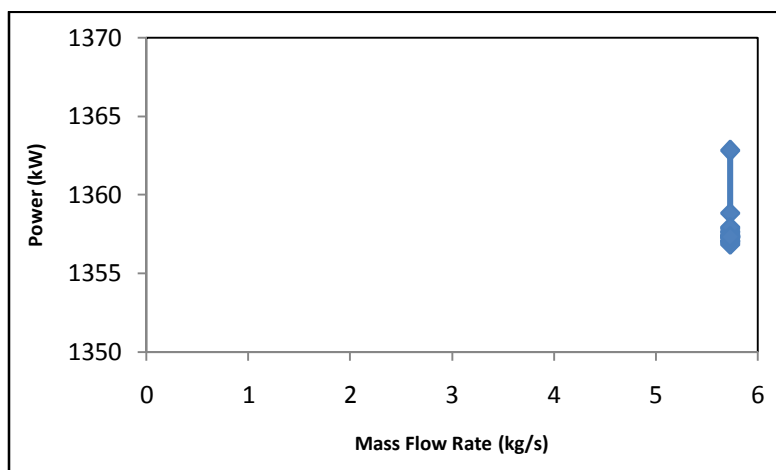


**Figure 20** Power versus Mass Flow

The impeller works with power a power requirement in the range of 1350 to 1360 kW on its 100 percent speed line over the range of total pressure ratio 4.5 to 5.4.

### 7.5. Validation Studies

The obtained results presented in the below figure shows state-of-the-art validity of current design with design performance work stated in [8].

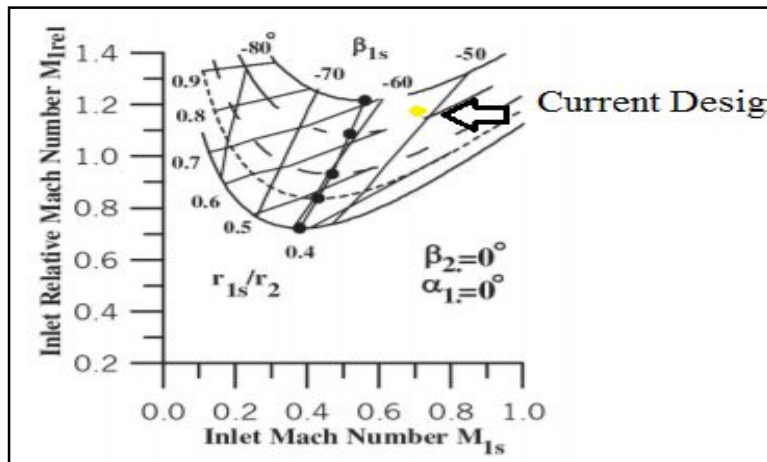


Figure 21 Comparison with compressor in [8]

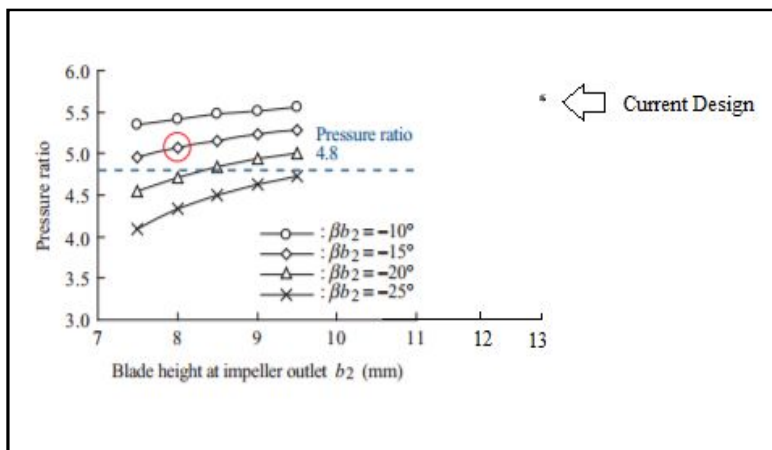


Figure 22 Comparison with trend established in Paper [9]

The design methodology adapted in current frame work uses a backswept angle of  $0^\circ$  and does not follow the design trend established for validation in above figure. Above deviations in the performance trends can be attributed to the structural size and rotational specifications of various stages.

### 8. CONCLUSION

The aero-thermodynamic design of centrifugal compressor turbo-machinery for a small gas turbine engine has been successfully carried out and sequentially investigated for its performance at design speed. The 3D computational analysis inferences that, the designed centrifugal compressor generates pressure ratio of 5.4 with an ingested mass flow rate of 5.73 kg/s at fixed rotational speed of 38000 rpm. The targeted flow parameters are in well agreement by centrifugal turbo-machinery within the diameter specification of 280, 340 mm for impeller and diffuser respectively. The total-to-total efficiency of designed centrifugal compressor is 81% against a target of 82%. The swirl at impeller is reduced from  $77^\circ$  to  $27.5^\circ$  by the diffuser thus reducing the primary losses viz., flow separation and thereby has the capability of experiencing lesser stall angles.

## REFERENCES

- [1] Philip P Walsh, Paul Fletcher. Gas Turbine Performance, 2<sup>nd</sup> Edition, John Wiley & Sons, pp. 178-186.
- [2] Cohen and Rogers. Gas Turbine Theory. Longman Group Limited, pp. 126-153.
- [3] Rama S.R. Gorla, Aijaz A. Khan. Turbomachinery: Design and Theory, CRC Press pp. 143-186.
- [4] David Gordon Wilson, Theodosios Korakianitis. The Design of High-Efficiency Turbomachinery and Gas Turbines, MIT Press, pp. 395-453.
- [5] P Dalbert, B Ribí, T Kmeci, M. V. Casey. Radial compressor design for industrial compressors. *Proceedings of the Institution of Mechanical Engineers, Part C: Journal of Mechanical Engineering Science*, 213(1), 1999, pp. 71-83
- [6] M.Ye. Deych and A.Ye. Zaryankin. Gas Dynamics and Exhaust Ducts of Turbo machines. Energiya, Moscow.
- [7] M V Casey and C J Robinson. A Guide to Turbocharger Compressor characteristics. Diesel motor entechnik, 10<sup>th</sup> Symposium, 30-31<sup>st</sup> March, Ostfilder. Ed. M. Bargende, TAE Esslingen, ISBN 3-924813-65-5, 2006.
- [8] Adnan Hamza Zahed and Nazih Noaman Bayomi. Design Procedure of Centrifugal Compressors. *ISESCO Journal of Science and Technology*, 10(17), 2014, pp. 77–91.
- [9] TAMAKI Hideaki, UNNO Masaru, KAWAKUBO Tomoki HIRATA. Aerodynamic Design of Centrifugal Compressor for AT14 Turbocharger. *IHI Engineering Review*, 43(2), 2010, pp. 70-76.
- [10] S.M. Swamy, V. Panndurangadu and J.M. Shamkumar. Effect of a Tip Clearance on the Performance of a Low Speed Centrifugal Compressor. *International Journal of Mechanical Engineering and Technology*, 8(1), 2017, pp. 178–188.